Supplementary Information: Two-dimensional Ambipolar Carriers of Giant Density at the Diamond/cubicBN (111) Interfaces: Toward Complementary Logic and Quantum Applications

Jiaduo Zhu[a], Kai Su[a], Zeyang Ren [a,b], Yao Li[c], Jinfeng Zhang[*,a,b], Jincheng Zhang[*,a],
Lixin Guo[d] and Yue Hao[*,a]

[a]*State Key Laboratory of Wide Bandgap Semiconductor Devices and Integrated Technology, School of Microelectronics, Xidian University, Xi'an 710071, China. E-mail: jfzhang@xidian.edu.cn, jchzhang@xidian.edu.cn, and yhao@xidian.edu.cn.*

[b]*Xidian-Wuhu Research Institute, Wuhu 241002, China.*

[c]*Department of Electronic Engineering, Xi'an University of Technology, Xi'an 710048, China.*

[d]*School of Physics, Xidian University, Xi'an 710071, China.*

1. Variation of band structure of cBN induced by lattice mismatch

Because diamond is usually adopted as a substrate for epitaxy growth, the in-plane lattice parameters were consistently set as that of the diamond (111) surface. The electronic structure of cBN can be influenced by the lattice mismatch of -1.43%. The effect was evaluated by fixing the in-plane lattice parameters of the unit-cell of cBN along [111] direction to that of diamond and allowing the out-plane lattice length and all the atoms to be fully relaxed. The band structure is shown in Fig. S1. Due to the hexagonal-like lattice of cBN along (111) direction, the high symmetry points are transferred from the cubic phase to the hexagonal lattice. The band gap of the strained cBN is 6.166 eV, slightly lower than that of 6.167 eV of the pristine cBN, which can be attributed to the small lattice mismatch.

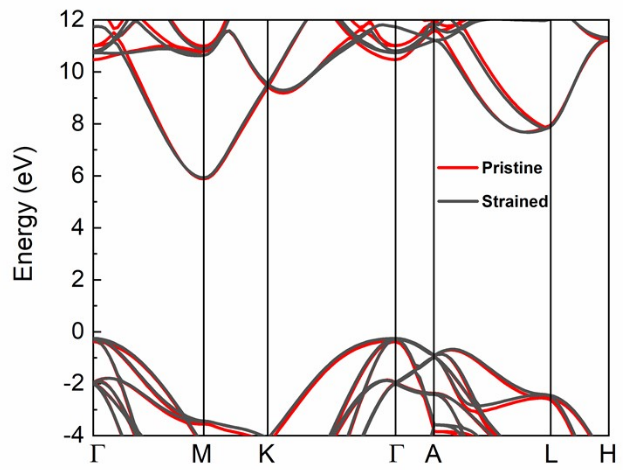

Fig. S1. Band structure of cBN unit-cell along [111] direction. The black and red denote pristine and strained cBN, respectively.

2. Stability evaluated by the molecular dynamics simulations

Molecular dynamics simulations were additionally performed for the structure of the lowest formation enthalpy. The NVT ensemble with the Nose-Hoover thermostat was adopted. The simulation was performed in two periods under varied temperatures. During the first period, the temperature gradually increased from 0 K to 600 K within 4000 fs at a timestep of 2 fs. The temperature then gradually decreased from 600 K to 300 K within another 4000 fs at the same timestep. The evolution of the temperature and total energy of the system as a function of time is presented in Fig. S2 below. We can notice from the snapshots of the structures that the bonds and atomic arrangement are stable with no distortion at various temperatures. The total energy of the systems also presents a regular oscillation scale following the temperature evolution.

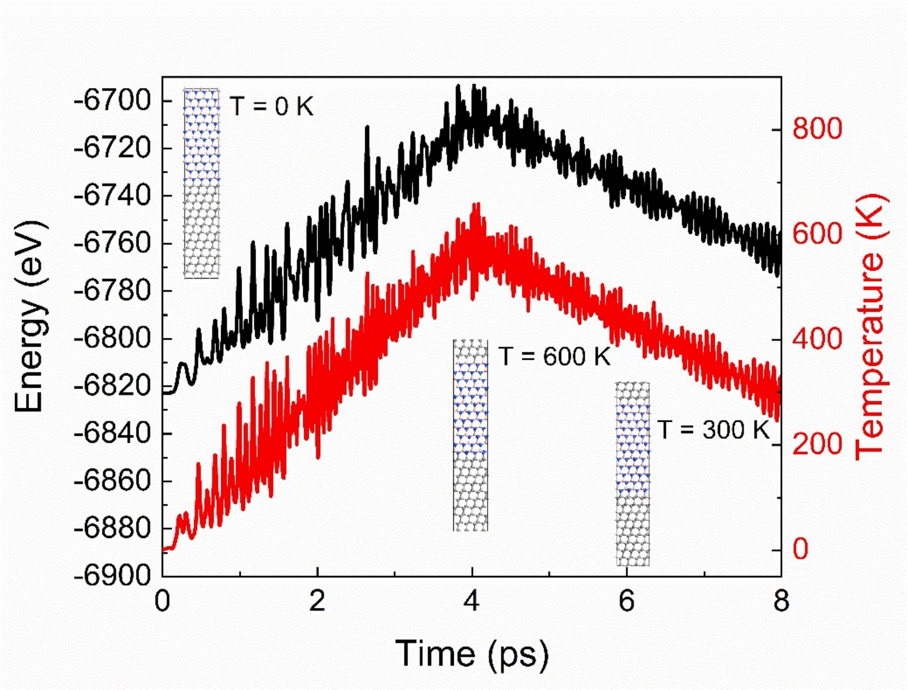

Fig. S2. Total energy and temperature of the Diamond_1DB/BN_1DB as a function of simulation time. The insets are the snapshots of atomic structure at the specific temperatures.

3. Detailed PLDOS at the band edges

Detailed PLDOS at the band edges was extracted and shown in Fig. S3. We can see that the shapes of DOS near band edges are triangle-like. The small plateau at the band edges is derived from the resolution limit, as the PLDOS as a function of coordinates is projected layer by layer of the atomic structures. As for holes, only the unoccupied states, which are above the Fermi level, correspond to the accumulated charge. As for the electrons, only the occupied states, which are below the Fermi level, correspond to the induced charge. Accordingly, the Fermi level with the triangle-like distribution of the DOS composes a triangular well, which confines all ionized charges.

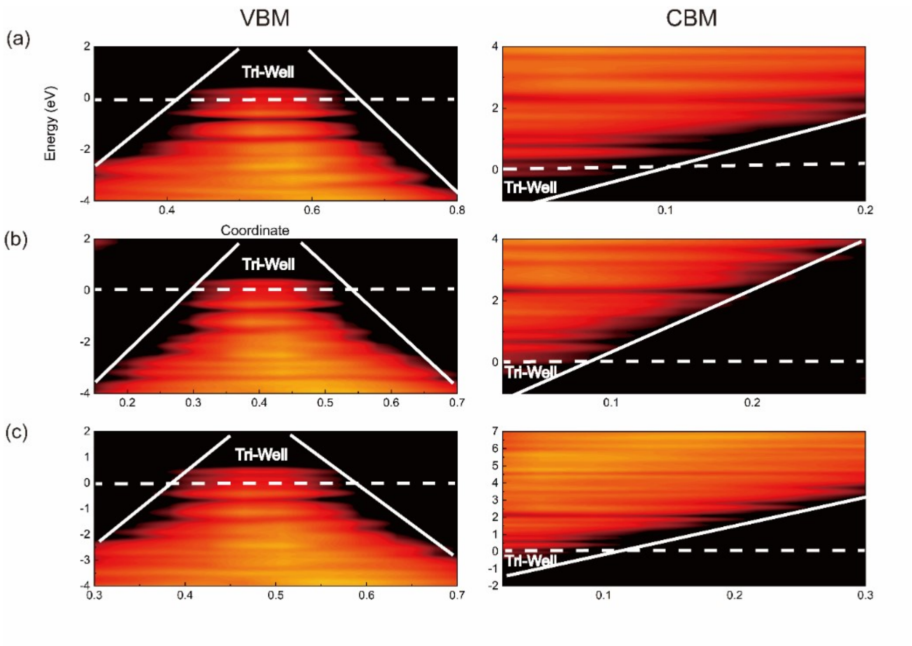

Fig. S3 Detailed PLDOS at the band edges for (a) Diamond_4U_BN_3U, (b) Diamond_3U_BN_4U, and (c) Diamond_4U_BN_4U. The left and right parts correspond to VBM and CBM, respectively. The dashed line is the Fermi level, and the solid line depicts the shape of the DOS near the band edges. The region of the triangular well is denoted as Tri-Well.

4. Electronic structure of Diamond_4U_BN_4U

As for the DOS shown in Fig. S4 (a), the bandgap is completely metalized similar to that of other systems. The band structure shown in Fig. S4 (b) is also analogous to other systems, in that the band dispersions near the Fermi level evolve in accordance with those in the other heterostructure, suggesting the common source of these bands. The occupied states exhibit little difference. In addition to the occupied CBM at the M, it can be noted that the conduction band at the K and H also becomes occupied as the thickness of diamond and BN increases from 3U to 4U, leading to an increase of the accumulated electron density. In response to the charge-neutral condition, the VBM gets raised slightly in reference to the Fermi level, more holes are accordingly induced. As for the PLDOS shown in Fig. S4 (c), the linear evolution of band edges as a function of coordinates is also in agreement with other structures. The VBM and CBM also correspond to the B-C and N-C interfaces, respectively. Obviously, the rise of the accumulated carriers at interfaces is derived from the gradual shift of band edges, which is proportional to the potential drop between the interfaces. If the built-in electric field does not diminish, increasing the cell's length can raise the potential drop, which is exactly observed in the diamond/BN heterostructures.

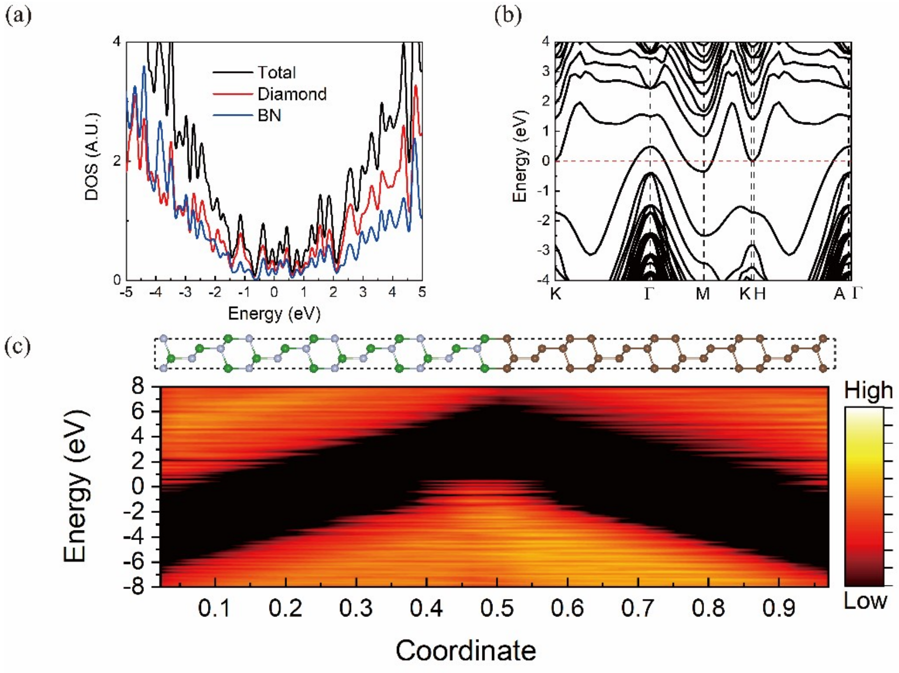

Fig. S4 (a) DOS, (b) band structure, and (c) PLDOS for Diamond_4U_BN_4U, respectively. The atomic structure is placed so that the atomic sites correspond to the coordinate.

5. The impact of terminals at cBN surface on the diamond/cBN heterojunction

As shown in Fig. S5 (a), the additional introduced boron and nitrogen layer induced monopoles at the interfaces. It can be noted that the potential increment at the boron termination (Coordinate = 51 Å) is higher than that at the nitrogen termination (Coordinate = 26 Å), a dipole is accordingly established between the two terminals. An electric field $E_{Surface}$ with direction from nitrogen to boron terminates (i.e. the [111] direction) is induced. However, another electric field E_{Bulk} can be obviously seen in the bulk part of cBN with a direction opposite to that of $E_{Surface}$. As shown in Fig. S5 (b), $E_{Surface}$ can only screen E_{Bulk} partially, the overall band bending of the heterojunction is still determined by the E_{Bulk}. Therefore, the hypothesis that 2D carriers are derived from asymmetrical terminations of cBN is not applicable to the diamond/cBN heterojunction.

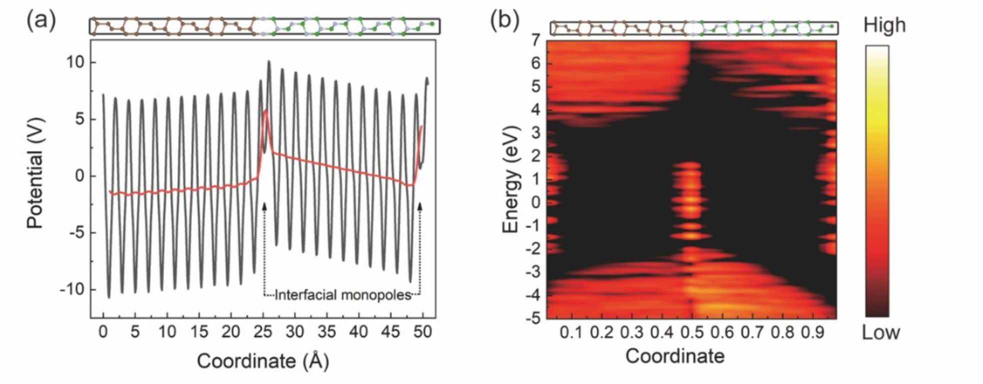

Fig. S5 (a) Electrostatic potential for Diamond_4U_BN_4U with additional N and B atoms attached to the cBN surfaces. The red lines are the average values in the materials. (b) The corresponding projected DOS. The Fermi level is at 0 eV. The color bar denotes the intensity of DOS.

6. The impact of cBN structural evolution on the potential in the heterojunction

To gain more insight into the origin of the polarization discontinuity, the effect of the atomic arrangement of BN on the electric field in the heterostructure is considered. The atoms of diamond were not allowed to move, and the cBN part was gradually transformed into a layered phase by aligning cations and anions to the same plane. A series of linearly interpolated images were built between heterostructures composed of pristine and layered cBN with diamond being fixed. For convenience, we introduced the "u", which is the ratio of the cation/anion separation along [111] direction of each image to that of the cBN phase, to represent the flatness of the layered cBN. With decreasing the "u" from 1 to 0, the cBN gradually evolves into the layered cBN with "ABC" stacking, which is different from the h-BN of "AB" stacking.

The averaged electrostatic potential of the insulating images is shown in Fig. S6 (a) and (b) for Diamond_4U_BN_1U and Diamond_1U_BN_4U, respectively. As seen from the potential evolution, flatting the BN layer (decreasing "u") gradually lowers the electric field strength in the bulk regions of both diamond and BN toward zero, leading to a simultaneous reduction of the bound charge. The transformation of cBN to the layered phase can gradually lower the overall electric field in the whole system, further indicating that the polarization discontinuity in the diamond/cBN heterostructures can be attributed to the non-vanishing formal polarization of cBN along the [111] direction.

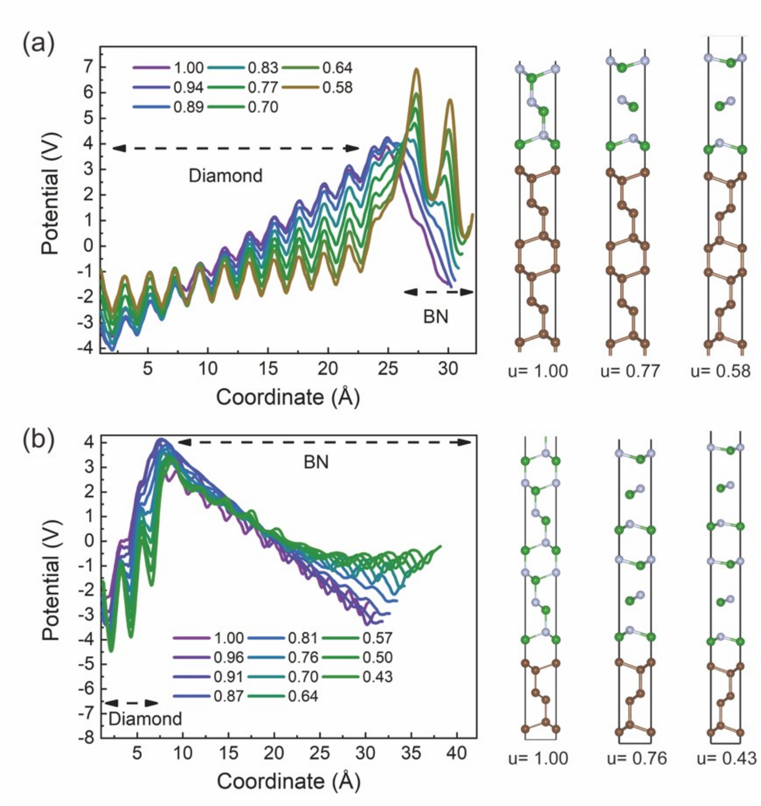

Fig. S6 (a, b) Averaged electrostatic potential of intermediate configurations for Diamond_4U_BN_1U and Diamond_1U_BN_4U, respectively. The right parts are the side views of typical configurations.